Infrared surface waves on semiconductor and conducting polymer

Monas Shahzad[1], Gautam Medhi[1], R. E. Peale[1], Ryuichi Tsuchikawa, Masahiro Ishigami[1], Walter Buchwald[2] and Justin Cleary[2], Glenn D. Boreman[3], Oliver Edwards[4] D. J. Diaz[5], and Ted. A. Gorman[5]

[1]Department of Physics, University of Central Florida, Orlando FL 32816, USA
[2]Air Force Research Lab, Sensors Directorate, Hanscom AFB MA 01731, USA
[3]College of Optics (CREOL), University of Central Florida, Orlando FL 32816, USA
[4]Zyberwear Inc., 2114 New Victor Rd., Ocoee, Florida 34761, USA
[5]Department of Chemistry, University of Central Florida, Orlando FL 32816, USA

ABSTRACT

Conductors with infrared plasma frequencies are potentially useful hosts of surface electromagnetic waves with sub-wavelength mode confinement for sensing applications. Such materials include semimetals, semiconductors, and conducting polymers. In this paper we present experimental and theoretical investigations of surface waves on doped silicon and the conducting polymer polyaniline (PANI). Resonant absorption features were measured in reflection from lamellar gratings made from doped silicon for various p-polarized CO_2 laser wavelengths. The angular reflectance spectra for doped silicon was calculated and compared with the experiments using experimental complex permittivities determined from infrared (IR) ellipsometry data. Polyaniline films were prepared, optical constants determined, and resonance spectra calculated also. A specific goal is to identify a conductor having tight mode confinement, sharp reflectivity resonances, and capability to be functionalized for biosensor applications.

Keywords: Infrared; Semiconductors; Conducting polymer; Gratings; Surface plasmons; Biosensor.

1. INTRODUCTION

Surface electromagnetic waves that propagate along the interface between a dielectric and a conductor exist at frequencies below the plasma frequency of the conducting material[1]. For these surface plasmon polaritons (SPP) to be bound with sub-wavelength confinement, the real part of the permittivity ε' should generally be negative and the imaginary part ε'' small. Qualitatively similar bound surface waves can occur above the plasma frequency when $\varepsilon'>0$ if $\varepsilon''>\varepsilon'$. For metals, like gold and silver, the first SPP situation holds for wavelengths in the visible and ultraviolet. For semi metals Bi and Sb, the latter condition holds throughout most of the mid IR.[2]

The principle commercial application of SPPs is in biosensors, where the change in the resonant coupling of light to SPPs gives information for identifying bio- molecules and quantifying their interactions. We hypothesize that potential sensitivity and selectivity advantages will accrue by operating SPP biosensors at wavelengths where biological analytes are strongly differentiated by their IR absorption spectra and where refractive indices are enhanced by dispersion[2,3]. This requires materials with plasma frequencies in the mid-IR. This paper investigates two such possible materials, heavily doped silicon and the conducting polymer polyaniline. The former allows all the advantages of silicon processing for making advanced sensor architectures. The latter allows spin coating, or even conformal dip-coating of non-planer sensors, for ultra-low cost processing.

2. EXPERIMENTAL DETAILS

Doped p-Si samples were commercially obtained and had specified resistivity ρ = 0.0006 - 0.001 ohm-cm, with carrier concentration N =1-2 X 10^{20} cm^{-3}. Lamellar gratings of 20 micron period, 50% duty, and various amplitudes were formed by standard photolithography. Profiles were confirmed using a step profilometer, e.g. Fig.1 (left).

Polyaniline was synthesized by making 1 mol /L aqueous HCl solution (pH between 0 and 2), ammonium persulfate as oxidant with an oxidant/ aniline (monomer) molar ratio $\leq$ 1.15 in order to obtain high conductivity and yield[4]. The monomer concentration was 0.1 mol/L. The solution temperature was 0°C in order to limit secondary reactions. The

duration of reaction was 2 h. Aqueous ammonium persulfate solution was added slowly drop by drop to the aniline/HCl solution. The mixture was stirred continuously during the whole reaction. The formed precipitate was removed by filtration and washed repeatedly with HCl and dried in an oven for 72 h. The obtained material was polyemeraldine salt, i.e. polyemeraldine hydrochloride (PANi-HCl), which has green color. It was secondary doped with 1 M aqueous solution of camphorsulfonic acid [CSA] [5] to increase conductivity. The obtained powder was washed and dried under vacuum for 48 h. Polyaniline (polyemeraldine) solutions of 10 and 16 wt % were prepared with solvent m-cresol. We spin-cast the polyaniline solution at 3000 and 2500 rpm for 0.5 and 1 min, respectively, to obtain different film thickness in different samples. Resistivity of the resulting film was measured using four contact method to be $\rho = 0.005\ \Omega$- cm.

To measure the infrared penetration depth, films of different thickness were deposited on un-doped double-side polished silicon. Transmission measurements were made using a Fourier spectrometer. Mechanical thickness was measured using atomic force microscopy near a scratch in the film. These measurements allowed us to determine the thickness needed in the subsequent ellipsometry measurements to avoid contributions from the substrate. Complex permittivities of doped p-Si and optically thick samples of polyaniline were determined using a J.A. Woollam IR-VASE in the wavelength range 1-40 micron.

Specular reflectance as a function of angle for doped p-silicon gratings was measured using a goniometer (Fig. 1, right), a line-tunable CO_2 laser, and a power meter Dips in the reflected power at certain angles on incidence indicate the excitation of SPPs.

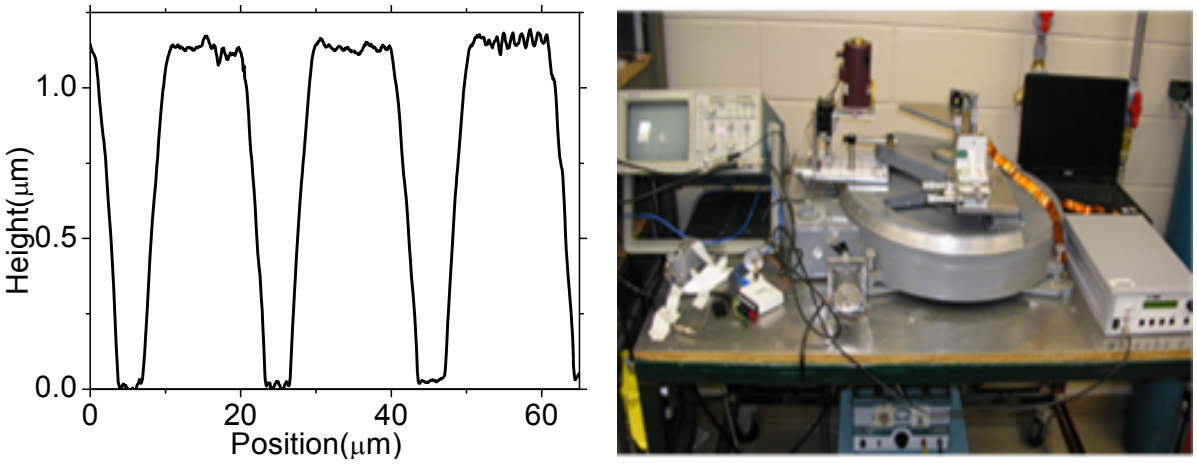

Fig.1 (left) Doped Silicon lamellar grating profile for grating with h = 1.12 μm. (right) Photograph of the experimental setup for measuring infrared specular reflection.

3. THEORETICAL CONSIDERATIONS

The raw ellipsometry outputs ψ and Δ are used to calculate complex permittivity $\varepsilon(\omega) = \varepsilon'(\omega) + i\,\varepsilon''(\omega)$ spectra based on standard Fresnel equations assuming an optically thick film[6]. The real amplitude of the complex reflectance ratio of p- to s-polarized light is tanψ, and Δ is the phase shift between the two reflected polarizations. At a given angle of incidence θ we have

$$\varepsilon' = \sin^2(\theta)\left[1 + \frac{\tan^2(\theta)\left(\cos^2(2\psi) - \sin^2(\Delta)\sin^2(2\psi)\right)}{\left(1+\sin(2\psi)\cos(\Delta)\right)^2}\right] \quad (1)$$

$$\varepsilon'' = \sin^2(\theta)\left[1 + \frac{\sin^2(\theta)\tan^2(\theta)\sin(4\psi)\sin(\Delta)}{(1+\sin(2\psi)\cos(\Delta))^2}\right] \tag{2}$$

The IR penetration depth into the conductor is

$$\delta = \frac{c}{\omega}\mathrm{Im}\left(\sqrt{\varepsilon}\right) \tag{3}$$

Gratings serve as couplers between photons and SPPs[7]. They function by shifting the incident photon wave vector by integer multiples m of 2π/p, where p is the grating period. The wave vector shift compensates for the inherent momentum mismatch between light and SPPs. Grating couplers allow multiple resonant SPP excitations to occur due to the multiple units of grating momentum that may be added to the incident wave vector. The coupling condition between an EM wave that is incident from the dielectric at an angle θ onto a grating and a SPP is

$$\eta_d \sin(\theta) + m\frac{\lambda}{p} = \pm\frac{c}{\omega}\mathrm{Re}\left[k_{spp}\right] \tag{4}$$

where m is an integer of either sign. The refractive index η_d of the dielectric above the grating is important in biosensing applications, since it changes and shifts the resonance angles due to surface binding of analyte molecules. In equation (4), the SPP wave vector k_{spp} is given in terms of the complex permittivity by

$$k_{spp} = \frac{\omega}{c}\sqrt{\frac{\varepsilon_d\varepsilon_c}{\varepsilon_d+\varepsilon_c}} \tag{5}$$

with c the light speed and ε_d, ε_c the complex permittivity of dielectric and conductor, respectively.

Calculation of angular reflection spectra was performed using the theory of Hessel and Oliner[7], [8] with a simplified model of the grating as sinusoidally modulated surface impedance with amplitude M. The average surface impedance relative to that of free space (337 Ω) is

$$\xi = -i\left(|\varepsilon'|^2 + \varepsilon''^2\right)^{-1/4}\left\{\cos\left(\frac{\phi}{2}\right) + i\sin\left(\frac{\phi}{2}\right)\right\} \tag{6}$$

where $\varphi = \tan^{-1}(\varepsilon''/\varepsilon')$. A coefficient D_n is defined as

$$D_n = \frac{2}{M}\left[1 + \frac{1}{\xi}\sqrt{1-\left(\sin\theta + \frac{n\lambda}{p\eta_d}\right)^2}\right] \tag{7}$$

where n is an integer and modulation parameter M is a function of grating permittivity, amplitude, and wavelength. For the calculations of this work, M is varied to fit measured data or to optimize the theoretical resonance line shape and strength. Finally, the specular reflectance of the grating is calculated by

$$R \approx \left|1 - \frac{4\cos\theta}{M\,\xi\left(D_0 - D_1^{-1} - D_{-1}^{-1}\right)}\right|^2 \tag{8}$$

The sinusoidal surface impedance approximation and the of D_n terms with $|n|>1$ gives calculated angular reflectance spectra in which only the m = 1 resonance appears.

The 1/e penetration depth of the electric field into the air above the conductor is give by

$$L_d = \left[\frac{\omega}{c} \mathrm{Re} \sqrt{\frac{-\varepsilon_d^2}{\varepsilon_d + \varepsilon_c}} \right]^{-1} \quad (9)$$

4. RESULTS

4.1 Doped silicon

Figure 2 presents permittivity spectra for heavy doped silicon from ellipsometry measurements. The ε′ values were negative below 0.2 eV, which corresponds to wavelengths longer than ~6 microns. The magnitude of imaginary part is larger than the magnitude of the real part, which is generally considered disadvantageous for SPP applications. In particular, the coupling resonances for conversion of free EM waves to SPPs at the grating surface are predicted to be broad, which we show experimentally to be the case, see below.

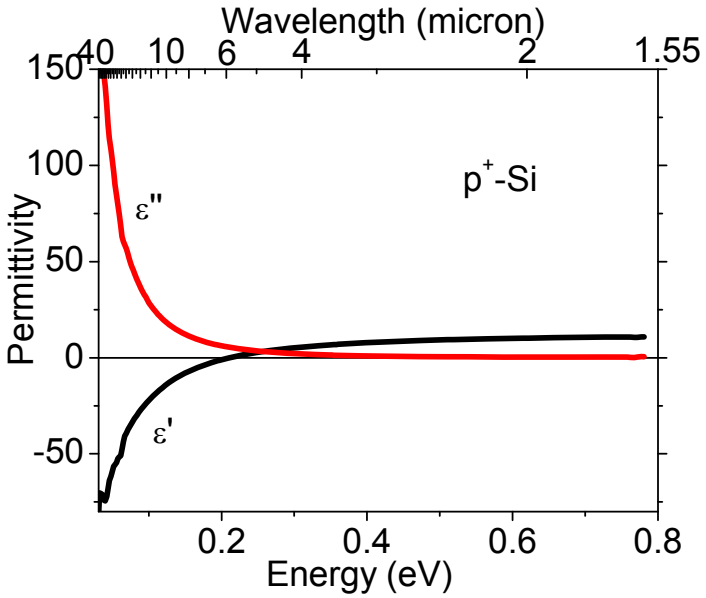

Fig. 2. Real and Imaginary part of permittivity for heavily-doped p-type silicon

The experimental permittivity values for doped p-Si at CO_2 laser wavelengths are given in Table 1, together with the relative surface impedance.

Table 1. Optical Parameters of Doped p-Si and Polyaniline

	λ (μm)	ε′	ε″	ξ[Eq.(6)]
p-Si	9.25	-11.4139	15.613	- *i* (0.2027 + i0.1028)
	10.59	-16.1949	20.9584	- *i* (0.1744 + i0.0856)
PANi	9.25	9.8848	20.04558	- *i* (0.1796 + i0.1116)
	10.59	11.51792	20.64031	- *i* (0.1773 + i0.1040)

Figure 3 presents the experimental reflected intensity as a function of angle of incidence at two different CO_2 laser wavelengths for silicon gratings of different amplitude *h*. For *h* = 0.45 micron, absorption resonances were barely discernable for the 10.59 micron wavelength, but they are lost in the baseline fluctuations for the 9.25 micron

wavelength. The resonances tend to get stronger up to about h = 1 micron, after which the broadening becomes more severe. The resonances are broad as was expected from the large ε″ values. The m = 1 resonance occurs at 34.45° and 29.60° for λ = 9.250 and 10.591 μm, respectively, as indicated by symbols and the labels "1". These values are in good agreement with those calculated from Eq. (4). Calculated resonance spectra are also plotted in Figure 3 together with the h = 1.12 μm data using M = 1 in Eq. (8). The agreement between experiment and theory is good. As mentioned above, only the m=1 resonance appears in the calculated curve because of the assumed sinusoidal impedance modulation with no higher harmonics.

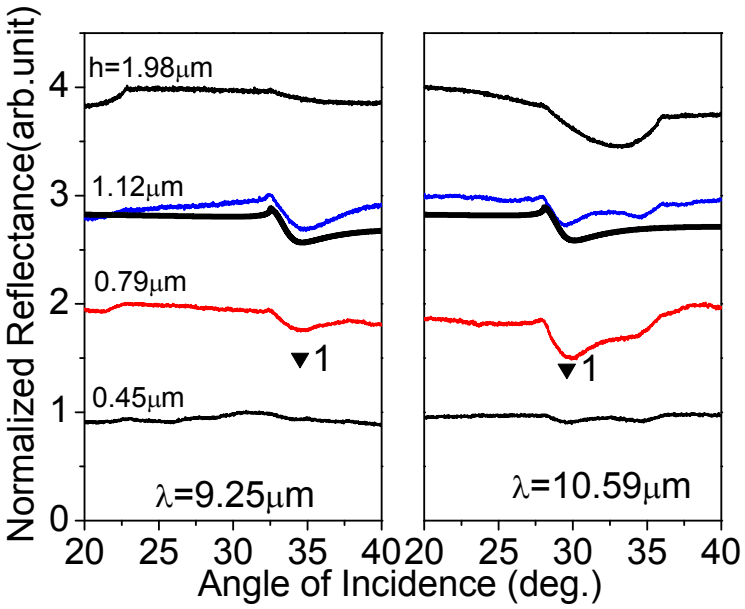

Fig. 3. Experimental angular reflectance spectra for heavily-doped p-Si lamellar gratings of 20 micron period of various amplitudes.

4.2 Polyaniline

Fig. 4 (left) shows the raw ellipsometry spectra (ψ, Δ) at an incidence angle of 65 deg. Figure 4 (right) presents permittivity spectra of polyaniline PANI-CSA calculated from the Fig. 4 (right) data (thick curves above the zero line). Data from Ref. [9] are plotted as symbols. Data for ε′ from Ref.[10] are plotted as a continuous curve that falls entirely below the zero line. Values of permittivity and surface impedance at our laser wavelengths are given in Table I. The ε′ values for our PANI-CSA sample were positive for all infrared wavelengths investigated, indicating lower than desired conductivity. The values are reasonable considering that the resistivity of our film is 5x higher than for our p-Si whose ε′ is barely negative at 10 μm.

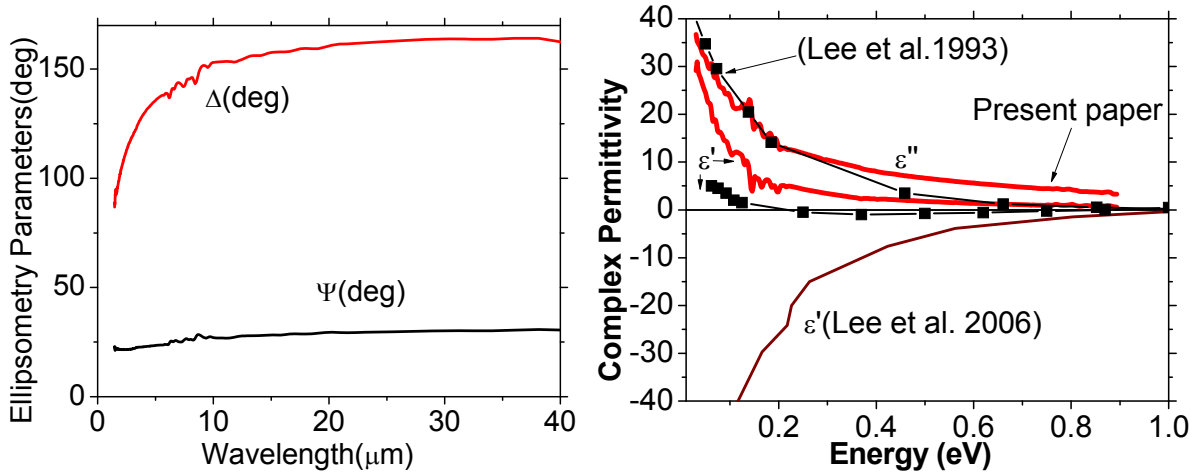

Fig. 4 (left) Raw ellipsometry data. (right) Real and imaginary part of permittivity for polyaniline from ellipsometry data, including published values from Refs. [9,10].

Ref. [9] values for ε′ are barely negative in the range 0.2 to 0.8 eV. Ref. [10] values go strongly negative for energies below 1 eV, which is characteristic of metallic behavior. (No ε″ spectrum is given in the later paper.) Our data are more closely in agreement with the Ref. [9] results, though our permittivity never goes negative. Both reports have $\varepsilon'' > \varepsilon'$ suggesting that useful SPP excitation resonances are still possible, though they may be broad. The resistivity of our sample is 0.005 Ω-cm which is higher than the values ρ = 0.000769 and 0.0029 Ω-cm from Refs. [9] and [10], respectively. It is curious that the most strongly negative ε′ data is for a sample intermediate in resistivity value. These results emphasize how variable conducting polymers can be in their optical properties.

The IR-field penetration depth into the conductor, δ, was determined using equation (3) to be ~4 microns at ~10 micron wavelengths. This value was qualitatively confirmed by FTIR spectrum of a spin-cast polyaniline film of 5 μm thickness on double side polished silicon. This transmission spectrum is presented in Figure 5 (left). The transmittance is almost zero across the middle infrared, in agreement with expectations from the estimated IR penetration depth.

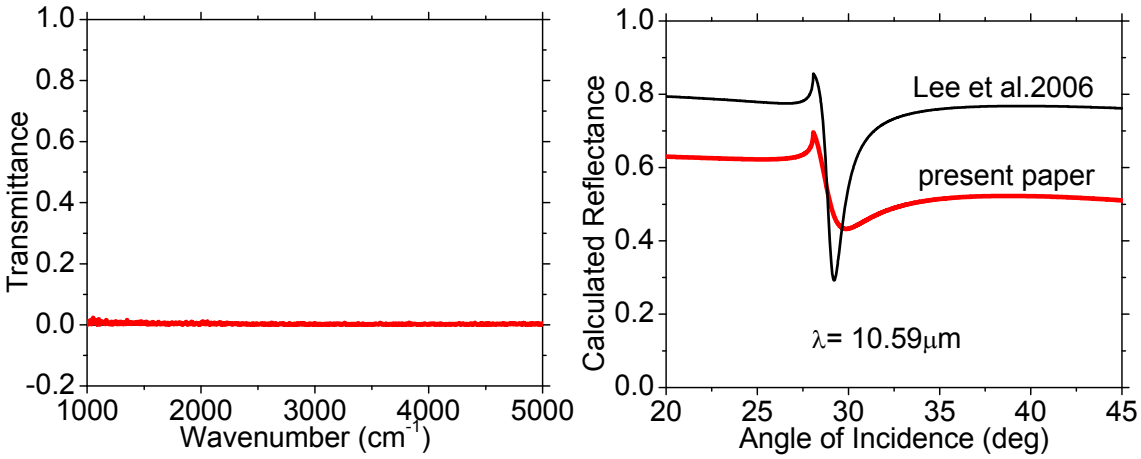

Fig. 5 (left) FTIR Spectrum of 5 μm thick Polyaniline Film (right) Comparison between calculated angular reflectance spectra of using our measured and the published[9] IR-ellipsometry data

Expected resonance angles and the angular reflectance spectra are calculated using the ε′ and ε″ values according to Eq. (8) using M =1. Figure 5 (right) presents the calculated reflectance spectra of SPPs for our measured and the published[9] permittivity values at λ = 10.59 μm. In both cases the ε′ value is slightly positive, yet SPP generation resonances are observed anyway because $\varepsilon'' > \varepsilon'$. The resonance based on ref. 9 data is sharper than the one based on our data. The

resonance angle for our measured permittivity is 29.65 deg which differs by 0.35 deg from the resonance angle determined using the published permittivity.

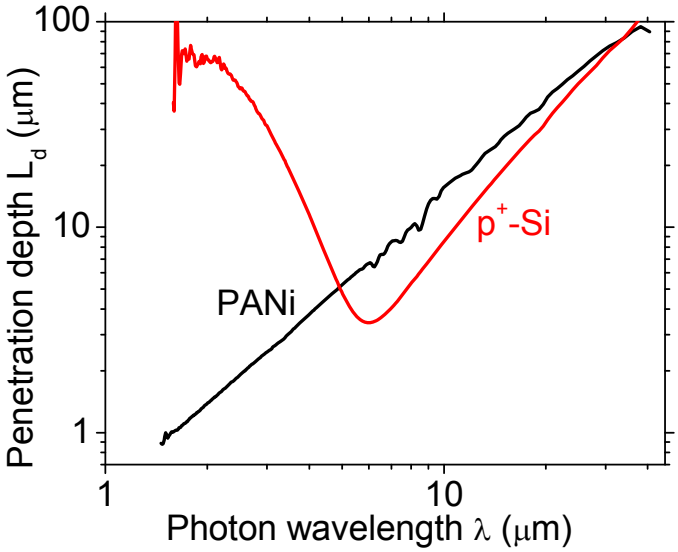

Fig. 6 Penetration depths versus free space wavelength.

Fig.6 presents the SPP field penetration depth above the conductor surface for both PANi and p^+-Si using our complex permittivity values and Eq.(9). PANi supports bound surface wave over the entire range 1-40 μm because $\varepsilon'' > \varepsilon'$ everywhere. For $\lambda > 10$ μm, the extent of the E-field above the surface starts to exceed the free space wavelength. For $\lambda < 10$ μm, the extent is slightly less.

For p^+-Si at $\lambda > 6$ μm, $\varepsilon' < 0$, so here this material supports a traditional SPP. The extent of the SPP is every where less for $6 < \lambda < 40$ μm. For $\lambda < 6$ μm, the p^+-Si has $\varepsilon' > 0$ and $\varepsilon'' \rightarrow 0$, and the material looks like a regular dielectric, which does not support a bound surface wave, and L_d quickly becomes >> λ.

5. SUMMARY

Calculated and experimental SPP resonances on heavily doped p-Si and calculated SPP-generation resonances on the conducting polymer polyaniline were presented. Both materials show resonances that should be sensitive to changes in the refractive index above their surfaces and hence should have potential to be used as the SPP hosts with sufficient mode confinement for IR sensor applications. Of the two materials, polyaniline promises to have the sharper, and hence more useful resonances. Additionally, polyaniline promises tight mode confinement over a broader range of IR wavelengths from 1-40 μm.

Acknowledgment

This work was supported by AFOSR grant number FA 95501010030, Gernot Pomrenke, Program Manager.

REFERENCES

[1] Maier S. A *Plasmonics: Fundamentals and Applications (Springer, 2007).*
[2] Cleary J. W, Peale R. E, Shelton D, Boreman G, Soref R, Buchwald W. "Silicides for Infrared Surface Plasmon Resonance Biosensors,". Proc. Mat. Res. Soc. 1133-AA10-03 (2008).
[3] Cleary J.W, Medhi G, Peale R.E, Buchwald W. R, Edwards O, and Oladeji I, "Infrared Surface Plasmon Resonance Biosensor", Proc. SPIE 7673, 5 (2010).
[4] Syed A. A, Dinesan M. K, "Polyaniline a novel polymeric material." Talanta 38, 815-837 (1991).
[5] Han M.G, Lee J , Byun S.W,. Im S.S "Physical properties and thermal transition of polyaniline film" Synth. Met. 124, 337 (2001).
[6] Tompkins H. G, *A user's guide to ellipsometry* (Academic, San Diego, 1993).
[7] Cleary J. W, Medhi G, Peale R. E, and Buchwald W. R, "Long-wave infrared surface plasmon grating coupler",. Appl. Optics 49, 3102 (2010).
[8] Hessel A. and Oliner A.A, "A new theory of Wood's anomalies on optical gratings," Appl.Opt. 4, 1275 (1965).
[9] Lee K, Heeger A.L, and Cao Y. "Reflectance of polyaniline protonated with camphor sulfonic acid: Disordered metal-insulator boundary", Phys. Rev. B 48, 14884 (1993).
[10] Lee K, Cho S, Park S.H, Heeger A.J, Lee. C. W and Lee S.H "Metallic transport in polyaniline" Nature 441, 4 (2006).